Accepted Manuscript

Tracking bio-hydrogen-mediated production of commodity chemicals from carbon dioxide and renewable electricity

Sebastià Puig, Ramon Ganigué, Pau Batlle-Vilanova, M. Dolors Balaguer, Lluís Bañeras, Jesús Colprim

PII: S0960-8524(16)31703-5
DOI: http://dx.doi.org/10.1016/j.biortech.2016.12.035
Reference: BITE 17411

To appear in: *Bioresource Technology*

Received Date: 16 September 2016
Revised Date: 8 December 2016
Accepted Date: 9 December 2016

Please cite this article as: Puig, S., Ganigué, R., Batlle-Vilanova, P., Dolors Balaguer, M., Bañeras, L., Colprim, J., Tracking bio-hydrogen-mediated production of commodity chemicals from carbon dioxide and renewable electricity, *Bioresource Technology* (2016), doi: http://dx.doi.org/10.1016/j.biortech.2016.12.035

Tracking bio-hydrogen-mediated production of commodity chemicals from carbon dioxide and renewable electricity

Sebastià Puig[1,†], Ramon Ganigué[1,2], Pau Batlle-Vilanova[1,3], M. Dolors Balaguer[1], Lluís Bañeras[4] and Jesús Colprim[1]

[1] LEQUIA, Institute of the Environment, University of Girona, Campus de Montilivi, Carrer Maria Aurèlia Capmany, 69. E-17003, Girona, Catalonia, Spain. E-mail: sebastia@lequia.udg.cat ; marilos@lequia.udg.cat; JColprim@lequia.udg.cat

[2] Centre of Microbial Ecology and Technology, Ghent University, Coupure Links 653, B-9000 Ghent, Belgium. E-mail: Ramon.Ganigue@UGent.be

[3] Department of Innovation and Technology, FCC Aqualia, Balmes Street, 36, 6th Floor, 08007 Barcelona, Spain. E-mail: pau.batlle@fcc.es

[4] Molecular Microbial Ecology Group, Institute of Aquatic Ecology, University of Girona, E-17071, Girona, Spain. E-mail: lluis.banyeras@udg.edu

[†] **Corresponding author** LEQUIA. Institute of the Environment. University of Girona. Campus Montilivi. Carrer Maria Aurèlia Capmany, 69, E-17003 Girona. Catalonia. Spain E-mail address: sebastia@lequia.udg.cat

Abstract

This study reveals that reduction of carbon dioxide (CO_2) to commodity chemicals can be functionally compartimentalized in bioelectrochemical systems. In the present example, a syntrophic consortium composed by H_2-producers (*Rhodobacter* sp.) in the biofilm is combined with carboxidotrophic *Clostridium* species, mainly found in the bulk liquid. The performance of these H_2-mediated electricity-driven systems could be tracked by the activity of a biological H_2 sensory protein identified at cathode potentials between -0.2V and -0.3V vs SHE. This seems to point out that such signal is not strain specific, but could be detected in any organism containing hydrogenases. Thus, the findings of this work open the door to the development of a biosensor application or soft sensors for monitoring such systems.

Keywords: bioelectrochemical systems; biofuels; CO_2 transformation; white biotechnology.

1. Introduction

Biological production of added-value products from carbon dioxide (CO_2) and renewable electricity is a promising approach to recycle a greenhouse gas into carbon-neutral commodity chemicals. However, this remains a nascent concept with limited proof-of-concept studies using either pure bacterial cultures(Nevin et al., 2011, 2010; Tremblay and Zhang, 2015) or mixed populations(Bajracharya et al., 2015; Batlle-Vilanova et al., 2016; Ganigué et al., 2015; Jourdin et al., 2015b, 2014; Kuroda and Watanabe, 1995; Marshall et al., 2013b, 2012, Mohanakrishna et al., 2016, 2015; Patil et al., 2015).

The production of H_2, either biological or electrocatalytic, plays a key role in H_2-mediated biological production as it governs the availability of reducing power, and thus the transformation of CO_2 to organic products (Agler et al., 2011; Blanchet et al., 2015). Recently, the role of H_2 as a mediator has been highlighted. Jourdin and co-workers showed biologically induced H_2 production at -0.85 V vs SHE and further utilisation by acetogens within the biofilm (Jourdin et al., 2016). In a second study, Blanchet et al. poised the cathode at two different potentials (-0.36 and -0.66 V vs SHE) to test the effect of H_2 in biological production of carbon-based commodities. Acetogenic activity was only observed at -0.66 V vs SHE, demonstrating the importance of H_2 as intermediate of biological production of carbon-based commodities (Blanchet et al., 2015). To date, acetate is the main product of bioelectrocatalysed reduction of CO_2. Recently, Ganigué and co-workers proved that butyrate and small amounts of ethanol and butanol can be produced using CO_2 as a sole carbon substrate (Ganigué et al., 2015). In the latter work, acetate was the initial product, and butyrate accumulation was observed three days after. Later on, the high concentrations of organic acids, low

fermentation pH, and the increase of available reducing power presumably led to the re-assimilation of acetate and butyrate and their conversion into ethanol and butanol.

As of today, continuous research efforts have allowed to characterize the different electron transfer mechanisms in bioanodes and to understand their function. However, little is known on the electron-transfer mechanisms in biological production of commodity chemicals from CO_2. In this work, we have characterized electrochemically and microbiologically different H_2-mediated electricity-driven systems for CO_2 capture and transformation into added value compounds (acetate, butyrate, ethanol and butanol) with the aim of providing a deeper understanding of these systems, and particularly on how electrons flow from a solid-state cathode to a terminal electron acceptor.

2. Materials and Methods

2.1 Bioelectrochemical systems

Four identical 240 mL two-chambered H-type bioelectrochemical systems (BES) were used in this study. Table S1 compares the maximum commodity chemicals produced in these systems. The differences between product concentrations and spectrum could be related to slight differences in the operational conditions applied (pH_2, CO_2 feast-famine conditions and pH). In all cases, anodic and cathodic chambers were separated by a cationic exchange membrane (CMI-7000, Membranes International Inc., USA), and maintained in constant stirring to avoid mass transfer limitations. Sampling ports and electrodes were housed in gas-tight butyl-rubber septa closing both anode and cathode compartments. Titanium rod (Ti plus 50 $g \cdot m^{-2}$ Pt, Magneto, The Netherlands) and carbon graphite (9 cm^2, NuVant's ELAT® LT2400W, FuelCellsEtc, USA) were used as anode and cathode electrodes, respectively. Net anodic and cathodic compartments

volumes were both set to 100 mL. BES were covered with aluminium foil throughout the experiment to prevent phototrophic activity.

Biocathodes were inoculated using 5 mL of an enriched carboxydotrophic mixed culture grown on syngas (32% CO, 32% H_2%, 8% CO_2 and 28% N_2) in a lab-scale reactor. This mixed culture exhibited a sustained production of C_2 and C_4 organic acids and alcohols(Ganigué et al., 2015). The inoculum was dominated by species of the genus *Clostridium: C. carboxidivorans/ C. ragsdalei/ C. kluyveri*. A synthetic medium containing 2-bromoethanesulfonate to inhibit methanogenesis was used in both anode and cathode (Ganigué et al., 2015). The synthetic medium was prepared with deionised water and contained per litre: 1 g KH2PO_4, 1 g NaCl, 0.25 g NH_4Cl, 0.25 g MgOH, 0.1 g KCl, 0.03 g $CaCl_2$. Additionally, 1 mL·L^{-1} of trace metal solution (concentration per litre: 20 g nitrilotriacetic acid, 10 g $MnSO_4 \cdot H_2O$, 8 g $Fe(SO_4)_2(NH_4)_2 \cdot 6H_2O$, 2 g $CoCl_2 \cdot 6H_2O$, 0.2 g $CuCl_2 \cdot 2H_2O$, 0.2g $NiCl_2 \cdot 2H_2O$, 0.2 g $Na_2MoO_4 \cdot 2H_2O$, 0.2 g Na_2SeO_4, 0.2 g Na_2WO_4, 2 mg $ZnSO_4 \cdot 7H_2O$), and 1 mL·L^{-1} of vitamin solution (concentration per litre: 100 mg Pyridoxine hydrochloride, 50 mg Thiamine hydrochloride, 50 mg Riboflavin, 50 mg Nicotinic acid, 50 mg DL-Calcium pantothenate, 50 mg p-Aminobenzoic acid, 50 mg Thioic acid, 20 mg Biotin, 20 mg Folic acid, 1 mg Vitamin B12), were added to the medium.

The temperature of all BES was maintained at 34±1ºC, and no pH control was applied. Pure CO_2 (Praxair, Spain) was sparged regularly every 2-3 days for a period of 5 minutes to warrant substrate availability. This sparging time ensured saturation of dissolved carbon (at 34ºC, concentration at saturation is 26.9 mM C-CO_2) as assayed regularly in control set-ups. Liquid samples (10 mL) were taken periodically (thrice a week, on average) from both anodes and cathodes for the monitoring of the concentration of

products and pH. The volume withdrawn was replaced with freshly prepared mineral medium.

2.2 Electrochemical instrumentation

A 5-channel potentiostat (BioLogic, Model VSP, France) was connected to the BES. Software from the same producer (EC-Lab v10.37) was used to run simultaneous multitechnique electrochemistry routines, which included chronoamperometry (CA), cyclic voltammetry (CV) and differential pulse voltammetry (DPV). A cathode potential (E_{cat}) of -0.8 V vs. SHE was used for CA. This potential was set at -0.8V vs. SHE to drive bioelectrocatalyzed reduction through H_2, following a similar strategy as that reported in recent publications (Bajracharya et al., 2015; Jourdin et al., 2015b; Marshall et al., 2013a; Patil et al., 2015). The cathodic potential was monitored with an Ag/AgCl reference electrode (0.197 V vs. SHE), model RE-5B BASi, United Kingdom). The parameters for CV were as follows: scan rate: 1 mV/s; E_i = -0.8 V vs. SHE; E_f= 0.0 V vs. SHE. Four CV cycles were performed in each routine, but only data from the last cycle is shown. The parameters for DPV were as follows: $E_{initial}$ (E_i)= 0.0 V vs. SHE and E_{final} (E_f)= -0.8 V vs. SHE; pulse height: 50 mV; pulse width: 300 ms; step height: 1 mV; step time: 1,000 ms; scan rate: 1 mV/s; current averaged over the last 20% of the step (1 s, 300 points). DPV and CV data were analysed with SOAS software(Fourmond et al., 2009) to identify the oxidation and reduction peaks.

2.3 Microcosms based experimentation

To further characterize the electrotrophic activity of the biocathode community, different experiments were carried out in four tailor-made single-chamber BES (microcosms) as described in Pous et al. (Pous et al., 2014). Each microcosm, with a final working volume of 14 mL, was composed of a graphite rod (Sofacel, Spain) with a

136 projected surface area of 7.85 cm^2 as a working electrode, a platinum wire as a counter
137 electrode and an Ag/AgCl reference electrode (model RE-5B BASi, United Kingdom). The
138 microcosms were also covered with aluminium foil throughout the experiment to
139 prevent phototrophic activity.
140
141 Two sets of experiments were carried out using a pure culture of *Rhodobacter*
142 *capsulatus* (DSM1710) and mixed cultures from BES 3 and 4. These experiments had
143 two aims: i) to demonstrate that a defined *Rhodobacter* culture could produce
144 hydrogen at the cathode and ii) to assign a role of the unidentified redox peak observed
145 in the electrochemical characterization of these systems. The working electrode of each
146 microcosm was operated chronoamperometrically at −0.8 V vs. SHE, the same cathode
147 potential poised at the parents BES. Pure CO_2 was flushed regularly every 2-3 days for 5
148 minutes to ensure substrate availability. Once a stable reductive current density was
149 reached, broth was replaced with fresh medium to remove planktonic cells and to
150 ensure observations were related only to the biofilm activity.
151 Experiments with a pure culture of *Rhodobacter capsulatus* (DSM1710) were
152 performed. Cultures were obtained from DSMZ (www.dsmz.de) and maintained at
153 recommended culturing conditions using mineral media DSM27 and ATCC1704 media.
154 Active cultures at early exponential conditions in 10 mL liquid media were used as
155 inocula for microcosm experiments. *Rhodobacter capsulatus* was inoculated and tested
156 for H_2 production and electroactive properties. Once the role of *Rhodobacter sp* was
157 elucidated, two microcosms were started-up using 5 mL of inoculum from the BES 3 and
158 4 cathodes and 9 mL of fresh medium were sequentially tested in dark-light transient
159 conditions to assess the activity of the Photosystem I. The microcosm was exposed 24
160 hours to illumination using a light-emitting diode (LED) (6.5W, 320lm, 50-60Hz, OSRAM
161 42706).

2.4 Analyses

The concentration of organic acids (acetate and butyrate) and alcohols (ethanol and butanol) were analysed using an Agilent 7890A gas chromatograph (Agilent, USA) equipped with a DB-FFAP column and a flame ionisation detector. The composition of the gas phase was analysed with an Agilent 7890A gas chromatograph (GC) equipped with an HP-Molesieve column and a thermal conductivity detector (TCD) to detect H_2, oxygen, nitrogen, methane, carbon monoxide and CO_2. The pH and conductivity were regularly measured from both effluents (pH-Meter Basic 20^+, EC-Meter Basic 20^+, Crison Instruments, Spain).

2.5 Determination of bacterial community structure

Bacterial communities from biofilm and bulk liquid samples were taken at day 36 of BES 4 and analyzed using conventional molecular methods. All four BES had the same inoculum. Samples were taken from BES 4 which produced carboxylates and alcohols (Table S1). Samples were collected aseptically using basic microbiological precautions in a continuous CO_2 from the biocathode. DNA was extracted using the FastDNA® SPIN kit for soils (MP, Biomedicals) following exactly manufacturer's instructions. DNA from biofilms was extracted directly from 0.5 cm^2 (projected surface) of carbon cloth. DNA of suspended cells was extracted from pelleted 4 mL samples. A preliminary PCR-DGGE analysis of samples was performed using the V3-V5 hypervariable region of the 16S rRNA gene as described previously (Prat et al., 2009; Vilajeliu-Pons et al., 2015) to check for differences among replicates.

Four replicates were selected for the analysis of the V1-V3 variable region of the 16S rRNA gene of Bacteria. Amplicons were obtained using the D88 (5'-

GAGAGTTTGATYMTGGCTCAG-3') and R519 (5'-ACCGCGGCTGCTGGCAC-3') universal primers. Barcodes and Illumina adaptors were fused to primers. Sequences were obtained with the Illumina MiSeq platform (paired-end method PE300) using conventionally adapted protocols. Sequencing was performed by DNA Vision (Gosselies, Belgium). Paired end sequences were joined and refined using QIIME (Quantitative Insights Into Microbial Ecology, v. 1.9.0) software package(Caporaso et al., 2010) with default parameters. Minimum sequence quality was set to q28 and only sequences with a minimum overlapping fragment of 25 bp were considered. A homogenous subset of sequences, corresponding to the lower number of sequences found in a single sample, was randomly obtained for each sample and used for comparisons. All comparisons between samples and taxonomic assignations were made using an Operational Taxonomic Unit (OTU) based approach at a similarity cutoff level of 97% (roughly at the species level). OTUs having less than 10 sequences were discarded from the analysis. Representative sequences for each OTU were assigned taxonomically using either QIIME (Green Genes dataset release gg_13_5_otus), or after Blast searches at the NCBI.

3. Results and discussion

3.1 Structure of the electrosynthetic microbiome

The microbial community of the biocathode had a rather low diversity with few clearly dominant phylotypes both at the biofilm and the bulk liquid samples (Shanon's diversity index < 2.0). A total of 48, 263 sequences were distributed selectively according to the sample type in 69 OTUs containing at least ten sequences. More than 80% of sequences (38,720 sequences) distributed in only ten OTUs, thus reinforcing the low diversity of the microbial community. This situation revealed a low functional redundancy in the BES, most likely related to the limited range of incubation conditions applied to the system(Konopka, 2009). Sequences were distributed mostly within the *Proteobacteria*

214 (65.9% of sequences) and the *Firmicutes* (29.8%) both in the bulk liquid and the biofilm
215 samples. However, significant differences of the microbial community structure
216 between the two sample types were observed at lower taxonomic levels (Weighted
217 Unifrac test, p<0.001, Figure 1). *Proteobacteria* distributed mainly within the
218 *Alphaproteobateria* in the biofilm sample but not in the bulk media, where
219 *Betaproteobacteria*, specifically the *Rhodocyclales*, appeared as the dominant
220 population. *Clostridiales* were the most abundant *Firmicutes* in both sample types.
221
222 Highly represented phylotypes of both sample types revealed interesting differences at
223 the genus and species level that suggested a functional compartmentalization of the
224 cathode cell (Table 1). Interestingly, highly differentiated populations in terms of
225 relative abundance between the two cell compartments included potentially
226 autotrophic bacteria representatives. Alphaproteobacteria accumulated in the cathode
227 surface, forming thick layers of low-diversity biofilms expanding over several
228 micrometres on top of the carbon cloth (Figure S1). All alphaproteobacteria belonged to
229 the Rhodobacteraceae and distributed in nine different OTUs. Eigth of them,
230 representing almost all alphaproteobacterial sequences found in the biofilm sample
231 (99.8%), showed a high similarity to either Paenirhodobacter enshiensis DW2-9^T (97.4%)
232 or Rhodobacter capsulatus SB1003 (96.8%). Unfortunately, no clear differentiation
233 between the two species could be obtained with the available sequence data.
234 *Rhodobacter* species and other Purple Nonsulfur Bacteria (PNB) have been proven as H_2
235 producers in anoxic conditions (Lubner et al., 2010). Net hydrogen production in
236 *Rhodobacter* sp. is mainly due to its nitrogenase activity and is essentially driven by light
237 through photosystem I (Smith, 2002). *Paenirhodobacter enshiensis* DW2-9^T has recently
238 been described as a non-pigmented cell within the Rhodobacteraceae. Unfortunately,
239 hydrogen production through nitrogenase activity has not been reported for this

240 species so far, but it is unlikely to occur via nitrogenase activity since no homologs of
241 *nifH*, *nifD* and *nifK* (the structural genes for nitrogen fixation) can be found in the
242 complete genome draft sequence (Wang et al., 2015).
243 Autotrophic *Firmicutes*, namely *Clostridium ljungdahlii* and *Clostridium*
244 *autoethanogenum* in view of 16S rRNA gene similarity, showed a completely different
245 distribution and accumulated almost exclusively in the bulk liquid. Carboxydotrophic
246 clostridia can fix CO and/or CO_2 into organic molecules through the Wood-Ljungdahl
247 pathway (Köpke et al., 2010), and excrete organic acids and alcohols as fermentation
248 products. An external source of reducing power, hydrogen or carbon monoxide in
249 conventional syngas fermentation is required for conversion of CO_2 as the sole carbon
250 source (Köpke et al., 2010). Based on the relative abundance of carboxydotrophs in
251 both bulk liquid and biofilm, it is plausible to assume that in the present system,
252 autotrophic conversion of CO_2 to organic matter may take place preferably in the bulk
253 liquid, and not in direct contact with the cathode surface. However, the latter cannot be
254 completely excluded as *C. ljungdahlii* , which has been proven to produce C_2 and small
255 amounts of C_4 electrotrophically(Nevin et al., 2011), was also detected in biofilm
256 samples.
257
258
259 *3.2 Electrochemical characterization*
260 Turnover cyclic voltammetries (CV) and differential pulse voltammetries (DPV) were
261 used to characterise electrochemically the BES capable to reduce CO_2 to organic acids
262 and alcohols. Figure 2 depicts two representative CVs under turnover conditions (in the
263 presence of CO_2), an abiotic control carried out before inoculation of bacteria, and a
264 second one in which C_2 and C_4 organic acids and small amounts of alcohols were
265 produced. Two redox pairs (differing significantly from the abiotic control) were

266 identified, one at -0.55 V vs SHE and the second one at -0.24V vs SHE. The redox pair at
267 -0.55V vs SHE is typically observed in H_2-producing biocathodes, in which the biofilm
268 catalyses this reduction, decreasing the important energy losses associated to the
269 catalytic hydrogen production (Batlle-Vilanova et al., 2014).
270
271 The second redox pair was identified at a formal potential of -0.244 V vs SHE at pH 4.63.
272 The anodic (E_{pA}) and cathodic (E_{pC}) peak potentials were -0.230 and -0.259 V vs SHE,
273 respectively. The peak separation ($\Delta E_p = E_{pA} - E_{pC}$) may allow the identification of the
274 mass-transfer regime(Harnisch and Freguia, 2012), and is often used as a criterion to
275 identify a reversible processes and fast charge exchange(Rieger, 1994). For reversible
276 redox couples controlled by diffusive mass transfer, the anodic and cathodic peak
277 potentials difference, ΔE_p, is always 0.059/z V at 25ºC, where z is the number of
278 electrons transferred in the half-reaction. The experimental ΔE_p was calculated as
279 0.028±0.005 V (n=10). According to a temperature-corrected ΔE_p of 0.061/z at 34ºC, 2
280 electrons were theoretically exchanged in this redox pair. A complementary calculation
281 of the number of electrons and protons exchanged in the reaction was done following
282 the methodology proposed by Bard and Faulkner(Bard and Faulkner, 2011), and
283 resulted in the involvement of 2 electrons and 1 proton.
284
285 *3.3 Relation between the redox pairs and the end-products*
286 DPV with small-amplitude pulses characterization offers better sensitivities compared
287 to normal pulse voltammetry (Bard and Faulkner, 2011), and were used to further
288 characterize the redox peak appearing at -0.244 V vs SHE. The correlation between pH-
289 value and the half-wave potential (Figure 3A), and between pH and peak intensity of
290 the half-wave potential (Figure 3B) was analysed experimentally. Results showed that
291 the formal potential of the redox-active pair was shifted towards a more positive value

292 with decreasing pH. The slope of the graph $E_{1/2}$ vs pH was -0.049 V per pH unit, close to
293 the theoretical value (0.061 V at 34ºC). This shift in the formal potential demonstrated
294 that the observed reduction reaction was proton dependent. The intensity of the half-
295 wave potential decreased at lower pHs from close to 0 A at pH 7 to $-1500 \cdot 10^{-6}$ A at pH 5
296 (Figure 3B), suggesting that electrotrophic activity was enhanced at lower pH values.
297 Figure 4 shows four representative DPVs obtained at different time points during the
298 experimental period, and at which CO_2 reduction yielded different end-products
299 (acetate, butyrate, ethanol and butanol). In all cases the reduction peak appeared at
300 around -0.24V vs SHE, shifting to more negative values at lower cathode pHs (Figure
301 3A). The peak was barely visible at the beginning of the experiment, when the
302 concentration of products in the broth was negligible, but it became clearly visible
303 when the production of organic acids and small amounts of alcohols started in the BES
304 (B, C and D). The intensity (area) of the peak increased as the cells produced longer
305 carbon-chain molecules and alcohols indicating higher levels of activity. It was, thus,
306 hypothesized that the redox peak area could be related to distinct metabolic reactions.
307
308 The comparison of the formal potential observed experimentally to the reduction
309 potential of several primary cofactors potentially involved in CO_2 transformation
310 pathways (Table 2) suggested that NADH and/or NADPH (E= -0.265 V and -0.269V vs
311 SHE at 34ºC and pH 5, respectively) could be involved in the reduction reactions
312 observed in the BES. NAD(P)H are biological electron carriers that play an important
313 role in maintaining the intracellular redox balance, and contribute to homeostasis in
314 microorganisms(Wang et al., 2013). These are intracellular cofactors and cannot be
315 detected using CVs and DPVs. However, NAD(P)H are involved in the different H_2
316 producing reaction in *Rhodobacter sp* (Lubner et al., 2010; Shafaat et al., 2013;

317 Swierczek et al., 2010; Tikhonov, 2014) , in photosystem, nitrogenases and
318 hydrogenases complexes.
319
320 *Rhodobacter* sp. typically have a group of hydrogenases and nitrogenases capable of
321 catalysing a reversible reduction of protons to hydrogen (Friedrich et al., 2011;
322 Geelhoed et al., 2010; Shafaat et al., 2013). In strictly anaerobic bacteria, Fd_{red}, NADH,
323 and cytochromes are the electron donors for the reduction of protons(Geelhoed et al.,
324 2010). These cofactors have similar reduction potentials to the redox pair
325 experimentally observed.
326
327
328 *3.4 Electrotrophy in bio-H_2-mediated* electricity-driven systems
329 Batch experiments were conducted in microcosms to gain further insights on the nature
330 and role of the unidentified redox peak. Each microcosm was inoculated using either a
331 pure culture of *Rhodobacter capsulatus* or fermentation broth from the cathodes of BES
332 3 and 4, respectively and poised at – 0.8 V vs SHE.
333 Two microcosms experiments with a pure culture of *Rhodobacter capsulatus* were done
334 to demonstrate that a defined *Rhodobacter sp* could produce hydrogen at the cathode
335 using electrons as electron donor. The electroactive properties of *Rhodobacter*
336 *capsulatus* were confirmed just after inoculation with concomitant current demand.
337 The electrons from the cathode electrode were taken by *Rhodobacter capsulatus* to
338 enhance the production of H_2 at a rate of 18.87 mmols $H_2 \cdot L^{-1} \cdot d^{-1}$ (coulombic efficiency:
339 60%).
340
341 Further electrochemical characterization (Figure 5) proved that the biofilm evolved to a
342 biological H_2 producing system. Moreover, the unidentified redox peak previously

observed in bioelectrochemical systems (Figure 4) also appeared shifted because of the pH difference. However, the low signal (area) observed associated to the low concentration of biomass present in these microcosms did not enabled further characterization of this pair. For this reason, experiments with mixed population from the BES 3 and 4 with higher biomass concentration were done.

CVs in mixed cultures microcosms were also performed before inoculation and after 95 hours of operation, once stable reductive current densities were reached (Figure S2). The redox pair between -0.2 and -0.3 V vs SHE was observed just after inoculation. The subsequent medium replacement to remove planktonic cells did not alter the characteristics of the redox peak, clearly indicating that this was linked to direct transfer of electrons from the solid state electrode to the cells firmly attached to the electrode and excluding any signal from an excreted metabolite. In this respect, the biocathodic biofilm was subsequently exposed to different conditions to elucidate if the observed peak could be related to photosystem, nitrogenases or hydrogenases activities.

The hypothesis that the peak was linked to the activity of the photosystem was tested in a microcosm by assessing the response of the biofilm to dark-light transient conditions. Results of DPVs (Figure 6) did not show any differences in the expression of the redox peak after exposing it to natural light or artificial light (320 lumens) for at least 24 hours, proving that H_2 producing was not light dependent. These results agree with the presence of *Paenirhodobacter* like bacteria in the cathode. *P. enshiensis* lacks photosynthetic membrane structures and pigments and grows chemoheterotrophically, while all *Rhodobacter* species known so far are photosynthetic (Wang et al., 2014).

Therefore, this redox pair could be related to the activity of nitrogenases and/or hydrogenases in *Rhodobacter* species. Phototrophs can also produce hydrogen through nitrogenases (Geelhoed et al., 2010), although and reduction of protons to H_2 by a nitrogenase will only take place in the absence of nitrogen or as a by-product of nitrogen fixation (Rivera-Ortiz and Burris, 1975; Smith, 2002). However, the medium used in this test contained ammonium, being this hypothesis unlikely. Duché et al., described that *Rhodobacter capsulatus* has another class of soluble, nonstandard [NiFe] hydrogenases (Duché et al., 2005). This membrane bound hydrogenase is the sensory or regulatory hydrogenase (RH). These proteins contain an active site similar to the Standard [NiFe] hydrogenases, exhibit high binding affinities for H_2, which allows them to mediate H_2-dependent signal transduction (Lubitz et al., 2014). However, these enzymes exhibit extremely low levels of activity, approximately 100-fold lower than the metabolic hydrogenases. Under reducing conditions or in the presence of hydrogen, the RH interacts as a homodimer with a histidine protein kinase for downstream regulation of metabolic hydrogenase protein transcription.

This [NiFe]-hydrogenase was also described by Bernhard and co-workers(Bernhard et al., 2001) as an H_2 sensor in the proteobacterium *Ralstonia eutropha*. The detection of physiologically important gases such as H_2 by organisms is mediated by biological sensors that convert the molecular signal into a cellular response (Bernhard et al., 2001). This signal could be used to track the performance of a bio-H_2-mediated production of commodity chemicals from CO_2 and renewable electricity. This redox pair signal reported in this study was also observed by others researchers (Jourdin et al., 2016, 2015a; Sharma et al., 2013) in autotrophic hydrogen-producing biofilms. Those biofilms were mainly composed by *Proteobacteria; Betaproteobacteria; Rhodocyclales and Rhodocyclaceae* detected in 16S rRNA analysis (Jourdin et al., 2015a) or

Curvibacter, Deltaproteobacteria, Desulfovibrionales, Desulfobacteraceae and *Syntrophobacteraceae* characterized by Flourescence in Situ Hybridization. This seems to point out that such signal is not strain specific, but could be detected in any organism containing a hydrogenase. Thus, the findings of this work open the door to the development of a biosensor application or soft sensors for monitoring such systems.

4. Conclusions

This study reveals: i) a syntrophic consortium in which an electro-active cathodic biofilm composed mainly by *Rhodobacter* sp. reduces protons to hydrogen, which is uptaken by the planktonic cells (i.e. *Clostidrium* sp.) to reduce carbon dioxide to organic acids and small amounts of alcohols; ii) *Rhodobacter* sp. could produce H_2 from the cathode electrode; and iii) the performance of H_2-mediated electricity-driven systems could be tracked by the activity of a biological H_2 sensory protein in *Rhodobacter* sp. identified at cathode potentials between -0.2 V and -0.3 V vs SHE.

Acknowledgements

The authors would like to thank the Spanish Ministry (CTQ2014-53718-R and CTM2013-43454-R) and the University of Girona (MPCUdG2016/137) for theirs financial support. LEQUIA and IEA have been recognised as consolidated research groups by the Catalan Government (2014-SGR-1168, and 2014-SGR-484). R.G. gratefully acknowledges support from Ghent University BOF postdoctoral fellowship (BOF15/PDO/068). P.B-V gratefully acknowledges the Catalan Government for the pre-doctoral grant received (2015FI-B2 00076).

420

421 **References**

422 1. Agler, M.T., Wrenn, B.A., Zinder, S.H., Angenent, L.T., 2011. Waste to bioproduct
423 conversion with undefined mixed cultures: the carboxylate platform. Trends
424 Biotechnol. 29, 70–8.
425 2. Bajracharya, S., ter Heijne, A., Dominguez Benetton, X., Vanbroekhoven, K., Buisman,
426 C.J.N., Strik, D.P.B.T.B., Pant, D., 2015. Carbon dioxide reduction by mixed and pure
427 cultures in microbial electrosynthesis using an assembly of graphite felt and stainless
428 steel as a cathode. Bioresour. Technol. 195, 14–24.
429 3. Bard, A.J., Faulkner, L.R., 2011. Electrochemical methods: Fundamentals and
430 Applications. John Wiley & Sons.
431 4. Batlle-Vilanova, P., Puig, S., Gonzalez-Olmos, R., Balaguer, M.D., Colprim, J., 2016.
432 Continuous acetate production through microbial electrosynthesis from CO2 with
433 microbial mixed culture. J. Chem. Technol. Biotechnol. 91, 921–927.
434 5. Batlle-Vilanova, P., Puig, S., Gonzalez-Olmos, R., Vilajeliu-Pons, A., Bañeras, L.,
435 Balaguer, M.D., Colprim, J., 2014. Assessment of biotic and abiotic graphite cathodes
436 for hydrogen production in microbial electrolysis cells. Int. J. Hydrogen Energy 39,
437 1297–1305.
438 6. Bernhard, M., Buhrke, T., Bleijlevens, B., De Lacey, A.L., Fernandez, V.M., Albracht,
439 S.P.J., Friedrich, B., 2001. The H2 sensor of Ralstonia eutropha: Biochemical
440 characteristics, spectroscopic properties, and its interaction with a histidine protein
441 kinase. J. Biol. Chem. 276, 15592–15597.
442 7. Blanchet, E.M., Duquenne, F., Rafrafi, Y., Etcheverry, L., Erable, B., Bergel, A., 2015.
443 Importance of the hydrogen route in up-scaling electrosynthesis for microbial CO2
444 reduction. Energy Environ. Sci. 3731–3744.

8. Caporaso, J.G., Kuczynski, J., Stombaugh, J., Bittinger, K., Bushman, F.D., Costello, E.K., Fierer, N., Peña, A.G., Goodrich, K., Gordon, J.I., Huttley, G.A., Kelley, S.T., Knights, D., Jeremy, E., Ley, R.E., Lozupone, C.A., Mcdonald, D., Muegge, B.D., Reeder, J., Sevinsky, J.R., Turnbaugh, P.J., Walters, W.A., 2010. QIIME allows analysis of high-throughput community sequencing data. Nat. Methods 7, 335–336.
9. Duché, O., Elsen, S., Cournac, L., Colbeau, A., 2005. Enlarging the gas access channel to the active site renders the regulatory hydrogenase HupUV of Rhodobacter capsulatus O2 sensitive without affecting its transductory activity. FEBS J. 272, 3899–3908.
10. Fourmond, V., Hoke, K., Heering, H. a, Baffert, C., Leroux, F., Bertrand, P., Léger, C., 2009. SOAS: a free program to analyze electrochemical data and other one-dimensional signals. Bioelectrochemistry 76, 141–7.
11. Friedrich, B., Fritsch, J., Lenz, O., 2011. Oxygen-tolerant hydrogenases in hydrogen-based technologies. Curr. Opin. Biotechnol. 22, 358–364.
12. Ganigué, R., Puig, S., Batlle-Vilanova, P., Balaguer, M.D., Colprim, J., 2015. Microbial electrosynthesis of butyrate from carbon dioxide. Chem. Commun. 51, 3235–3238.
13. Geelhoed, J.S., Hamelers, H.V., Stams, A.J., 2010. Electricity-mediated biological hydrogen production. Curr. Opin. Microbiol. 13, 307–315.
14. Harnisch, F., Freguia, S., 2012. A basic tutorial on cyclic voltammetry for the investigation of electroactive microbial biofilms. Chem. Asian J. 7, 466–75.
15. Hoelzle, R.D., Virdis, B., Batstone, D.J., 2014. Regulation mechanisms in mixed and pure culture microbial fermentation. Biotechnol. Bioeng. 111, 1–37.
16. Jourdin, L., Freguia, S., Donose, B.C., Chen, J., Wallace, G.G., Keller, J., Flexer, V., 2014. A novel carbon nanotube modified scaffold as an efficient biocathode material for improved microbial electrosynthesis. J. Mater. Chem. A 2, 13093.
17. Jourdin, L., Freguia, S., Donose, B.C., Keller, J., 2015a. Autotrophic hydrogen-producing biofilm growth sustained by a cathode as the sole electron and energy source.

Bioelectrochemistry 102, 56–63.

18. Jourdin, L., Grieger, T., Monetti, J., Flexer, V., Freguia, S., Lu, Y., Chen, J., Romano, M., Wallace, G.G., Keller, J., 2015b. High Acetic Acid Production Rate Obtained by Microbial Electrosynthesis from Carbon Dioxide. Environ. Sci. Technol. 49, 13566−13574.
19. Jourdin, L., Lu, Y., Flexer, V., Keller, J., Freguia, S., 2016. Biologically Induced Hydrogen Production Drives High Rate/High Efficiency Microbial Electrosynthesis of Acetate from Carbon Dioxide. ChemElectroChem 3, 581–591.
20. Konopka, A., 2009. What is microbial community ecology? ISME J. 3, 1223–30.
21. Köpke, M., Held, C., Hujer, S., Liesegang, H., Wiezer, A., Wollherr, A., Ehrenreich, A., Liebl, W., Gottschalk, G., Dürre, P., 2010. Clostridium ljungdahlii represents a microbial production platform based on syngas. Proc. Natl. Acad. Sci. U. S. A. 107, 13087–92.
22. Kuroda, M., Watanabe, T., 1995. CO2 reduction to methane and acetate using a bio-electroreactor with immobilized methanogens and homoacetogens on electrodes. Energy Convers. Manag. 36, 787–790.
23. Lubitz, W., Ogata, H., Ru, O., Reijerse, E., 2014. Hydrogenases. Chem. Rev. 114, 4081–4148.
24. Lubner, C.E., Grimme, R., Bryant, D.A., Golbeck, J.H., 2010. Wiring photosystem I for direct solar hydrogen production. Biochemistry 49, 404–414.
25. Marshall, C.W., LaBelle, E. V, May, H.D., 2013a. Production of fuels and chemicals from waste by microbiomes. Curr. Opin. Biotechnol. 24, 391–7.
26. Marshall, C.W., Ross, D.E., Fichot, E.B., Norman, R.S., May, H.D., 2013b. Long-term Operation of Microbial Electrosynthesis Systems Improves Acetate Production by Autotrophic Microbiomes. Environ. Sci. Technol. 47, 6023–9.
27. Marshall, C.W., Ross, D.E., Fichot, E.B., Norman, R.S., May, H.D., 2012. Electrosynthesis of commodity chemicals by an autotrophic microbial community. Appl. Environ.

497 Microbiol. 78, 8412–20.
498 28. Mohanakrishna, G., Seelam, J.S., Vanbroekhoven, K., 2015. An enriched electroactive
499 homoacetogenic biocathode for the microbial electrosynthesis of acetate through
500 carbon dioxide reduction. Faraday Discuss. 183, 445–462.
501 29. Mohanakrishna, G., Vanbroekhoven, K., Pant, D., 2016. Imperative role of applied
502 potential and inorganic carbon source on acetate production through microbial
503 electrosynthesis. J. CO2 Util. 15, 57–64.
504 30. Nevin, K.P., Hensley, S. a, Franks, A.E., Summers, Z.M., Ou, J., Woodard, T.L.,
505 Snoeyenbos-West, O.L., Lovley, D.R., 2011. Electrosynthesis of organic compounds
506 from carbon dioxide is catalyzed by a diversity of acetogenic microorganisms. Appl.
507 Environ. Microbiol. 77, 2882–6.
508 31. Nevin, K.P., Woodard, T.L., Franks, A.E., 2010. Microbial Electrosynthesis : Feeding
509 Microbial Electrosynthesis : Feeding Microbes Electricity To Convert Carbon Dioxide
510 and Water to Multicarbon Extracellular Organic. MBio 1, 1–4.
511 32. Patil, S., Arends, J.B., Vanwonterghem, I., van Meerbergen, J., Guo, K., Tyson, G.W.,
512 Rabaey, K., 2015. Selective Enrichment Establishes a Stable Performing Community for
513 Microbial Electrosynthesis of Acetate from CO2. Environ. Sci. Technol. 49, 8833–8843.
514 33. Pous, N., Koch, C., Colprim, J., Puig, S., Harnisch, F., 2014. Extracellular electron
515 transfer of biocathodes: Revealing the potentials for nitrate and nitrite reduction of
516 denitrifying microbiomes dominated by Thiobacillus sp. Electrochem. commun. 49, 93–
517 97.
518 34. Prat, C., Ruiz-Rueda, O., Trias, R., Anticó, E., Capone, D., Sefton, M., Bañeras, L., 2009.
519 Molecular fingerprinting by PCR-denaturing gradient gel electrophoresis reveals
520 differences in the levels of microbial diversity for musty-earthy tainted corks. Appl.
521 Environ. Microbiol. 75, 1922–1931.
522 35. Rieger, H., 1994. Electrochemistry. Chapman & Hall.

36. Rivera-Ortiz, J.M., Burris, R.H., 1975. Interactions among substrates and inhibitors of Interactions Among Substrates and Inhibitors of Nitrogenase. J. Bacteriol. 123, 537–545.

37. Shafaat, H.S., Rüdiger, O., Ogata, H., Lubitz, W., 2013. [NiFe] hydrogenases: A common active site for hydrogen metabolism under diverse conditions. Biochim. Biophys. Acta - Bioenerg. 1827, 986–1002.

38. Sharma, M., Aryal, N., Sarma, P.M., Vanbroekhoven, K., Lal, B., Benetton, X.D., Pant, D., 2013. Bioelectrocatalyzed reduction of acetic and butyric acids via direct electron transfer using a mixed culture of sulfate-reducers drives electrosynthesis of alcohols and acetone. Chem. Commun. (Camb). 49, 6495–7.

39. Smith, B.E., 2002. Structure. Nitrogenase reveals its inner secrets. Science 297, 1654–1655.

40. Swierczek, M., Cieluch, E., Sarewicz, M., Borek, A., Moser, C.C., Dutton, P.L., Osyczka, A., 2010. An electronic bus bar lies in the core of cytochrome bc1. Science 329, 451–454.

41. Thauer, R.K., Jungermann, K., Decker, K., 1977. Energy conservation in chemotrophic anaerobic bacteria. Bacteriol. Rev. 41, 809.

42. Tikhonov, A.N., 2014. The cytochrome b6f complex at the crossroad of photosynthetic electron transport pathways. Plant Physiol. Biochem. 81, 163–183.

43. Tremblay, P.-L., Zhang, T., 2015. Electrifying microbes for the production of chemicals. Front. Microbiol. 6, 1–10.

44. Vilajeliu-Pons, A., Puig, S., Pous, N., Salcedo-Dávila, I., Bañeras, L., Balaguer, M.D., Colprim, J., 2015. Microbiome characterisation of MFCs used for the treatment of swine manure. J. Hazard. Mater. 288, 60–68.

45. Wang, D., Liu, H., Zheng, S., Wang, G., 2014. Paenirhodobacter enshiensis gen. nov., sp. nov., a non-photosynthetic bacterium isolated from soil, and emended descriptions of

549 the genera Rhodobacter and Haematobacter. Int. J. Syst. Evol. Microbiol. 551–558.
550 46. Wang, D., Zhu, F., Zhu, X., Zheng, S., Wang, R., Wang, G., 2015. Draft genomic
551 sequence of a selenite-reducing bacterium, Paenirhodobacter enshiensis DW2-9(T).
552 Stand. Genomic Sci. 10, 38.
553 47. Wang, Y., San, K.Y., Bennett, G.N., 2013. Cofactor engineering for advancing chemical
554 biotechnology. Curr. Opin. Biotechnol. 24, 994–999.

555

556

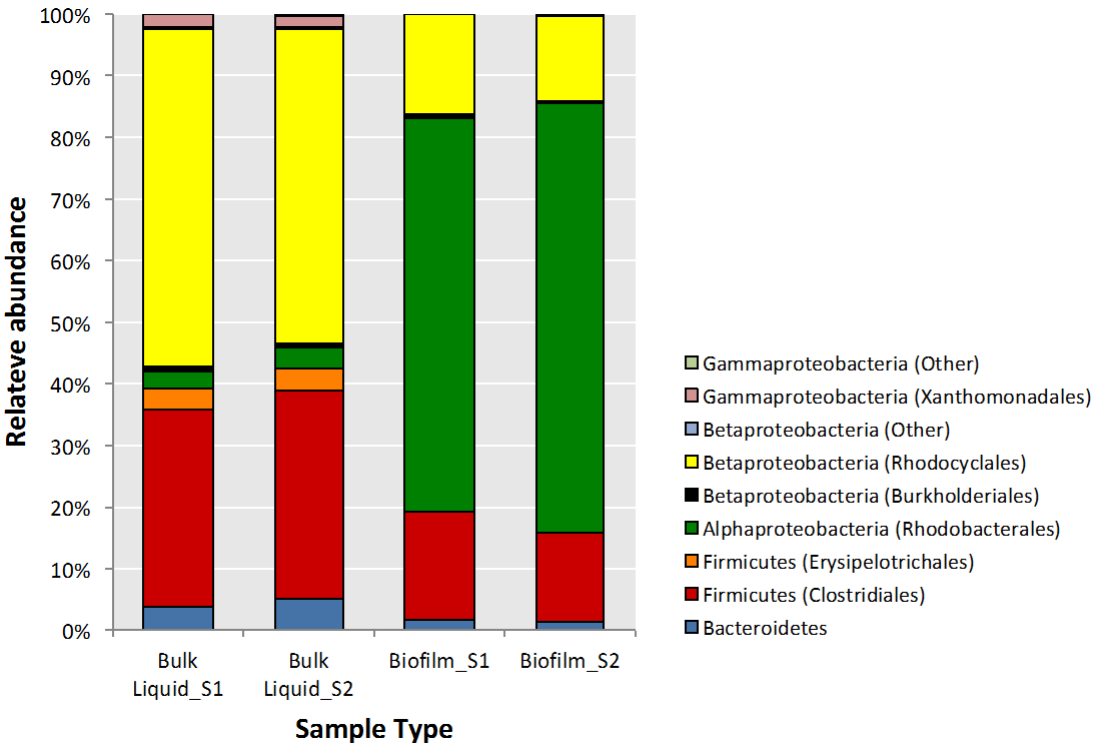

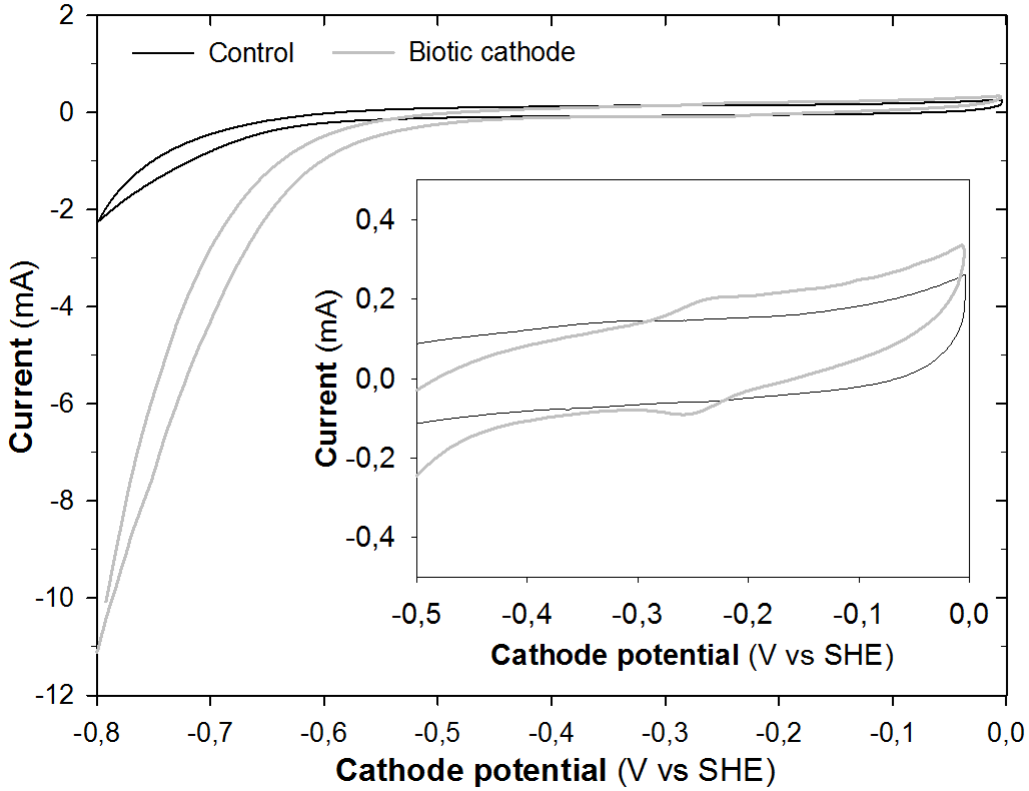

Figure 2. Turnover cyclic voltammograms under abiotic (devoid of cells, black line) and biotic (in the presence of a biofilm, grey) conditions. The scan rate was 1 mV s^{-1}.

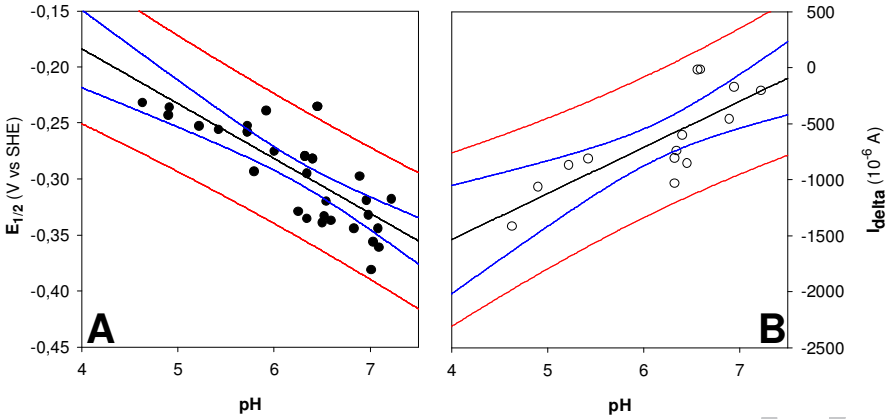

Figure 3. A) Correlation between pH-value and the half-wave potential ($E_{1/2}$), and B) correlation between pH and peak intensity of the half-wave potential. Determination done using DPV technique. Scan rate: 1 $mV \cdot s^{-1}$ and pulse height: 50mV. The regression line (in black) with 95% confidence band (in blue) and with 95% prediction band (in red) were calculated for the experimental data.

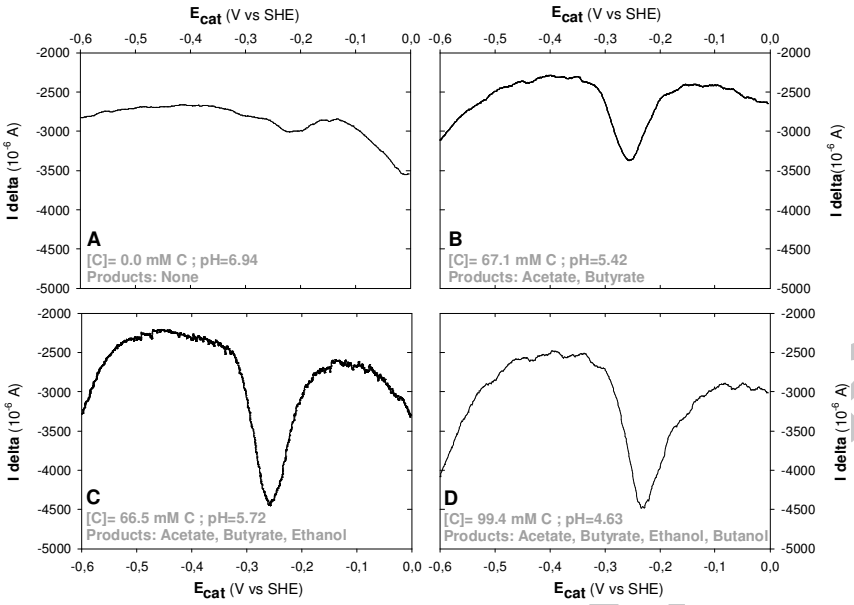

Figure 4. Representative DPVs (scan rate: 1 $mV \cdot s^{-1}$; pulse height: 50mV) during the experimental period with different added value production (acetate, butyrate, ethanol and butanol) from CO_2. [C]: Concentration of carbon.

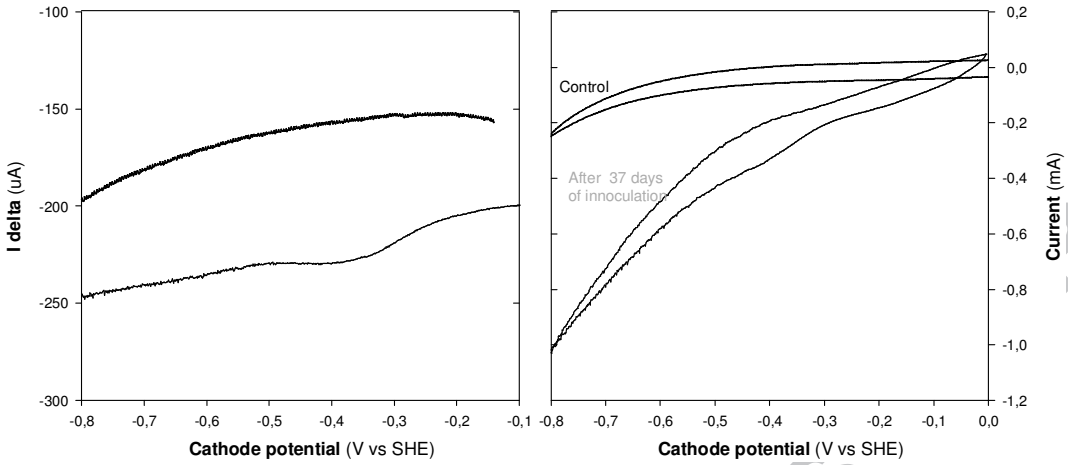

Figure 5. Representative DPVs (scan rate: 1 mV· s^{-1}; pulse height: 50mV; left) and turnover CVs (scan rate: 5 mV· s^{-1}; right) during the experimental period (before (black) and 37 days after the inoculation (grey)) of the microcosms with *Rhodobacter capsulatus*.

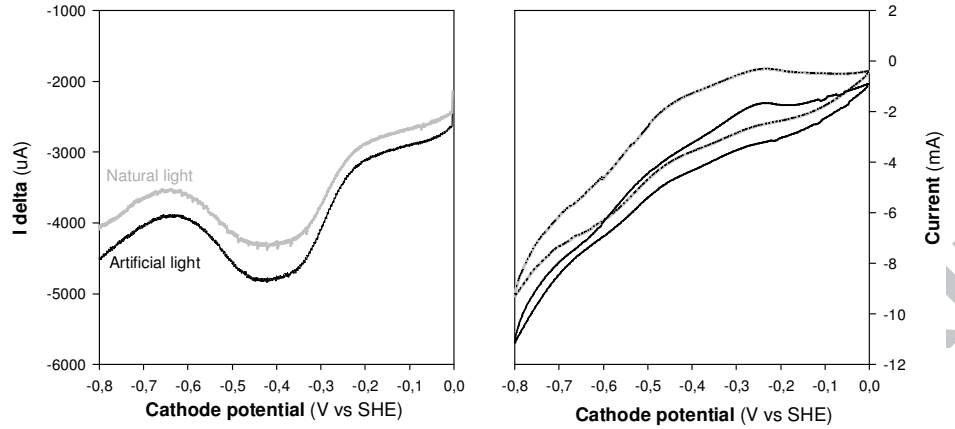

Figure 6. Representative DPVs (scan rate: 1 mV· s^{-1}; pulse height: 50mV; left) and turnover CVs (scan rate: 5 mV· s^{-1}; right) during the experimental period with natural light (grey) and artificial light (black) of the microcosms.

Most probable Identification (% similarity)	Sequence Similarity Range (%)	Number of OTUs	Relative abundance			
(% of sequences)						
			Bulk liquid_ S1	**Bulk liquid_ S2**	**Biofilm_**	
S1	**Biofilm_**					
S2						
Bacteroidetes						
(NR_041278) *Bacteroides coprocola* strain M16	88.5	1	3.8	5.1	1.8	1.2
Firmicutes						
(NR_117443) *Clostridium ljungdahlii* strain ATCC 55383	98.0-97.0	2	14.6	17.8	1.7	1.5
(NR_044849) *Clostridium thermobutyricum* strain JW171K	92.7-92.4	2	8.3	9.7	1.8	2.0
(NR_042516) *Clostridium nitrophenolicum* strain 1D	98.4	1	<0.1	<0.1	3.6	2.7
(NR_116828) *Paenibacillus prosopidis* strain PW21	81.0	1	2.8	1.6	ND	ND
Alphaproteobacteria						
(NR_125604) *Paenirhodobacter enshiensis* strain DW2-9	97.0	1	1.8	3.3	52.8	58.3
Betaproteobacteria						
(NR_074103) *Dechlorosoma suillum* strain PS	95.2	4	50.1	51.4	14.0	11.9
Gammaproteobacteria						
(NR_132712) *Pseudoxanthomonas jiangsuensis* strain wax	93.1	OTU9	1.6	0.9	ND	ND

Table 2. Reduction potentials (ΔE) in volts (vs SHE) of primary cofactors. Data was taken from *Hoelzle et al.(Hoelzle et al., 2014) and tThauer et al.(Thauer et al., 1977).

Temperature→	T=25ºC	T=34ºC				
Haft-reaction↓	pH=7	pH=4,5	pH=5	pH=6	pH=7	pH=8
*Cyt. C(Fe^{3+}) +e^-→Cyt. C (Fe^{2+})	0.223	0.223	0.223	0.223	0.223	0.223
tFMN + $2H^+$+$2e^-$→$FMNH_2$	-0.190	-0.049	-0.079	-0.140	-0.201	-0.262
tFAD+ $2H^+$+$2e^-$→$FADH_2$	-0.220	-0.079	-0.109	-0.170	-0.231	-0.292
*NAD^+ + H^++$2e^-$→NADH	-0.320	-0.250	-0.265	-0.296	-0.326	-0.357
*$NADP^+$ + H^++$2e^-$→NADPH	-0.324	-0.254	-0.269	-0.300	-0.330	-0.361
tFd +$2e^-$→Fd^{2-}	-0.401	-0.401	-0.401	-0.401	-0.401	-0.401

List of Figures:

List of Tables:

Graphical Abstract

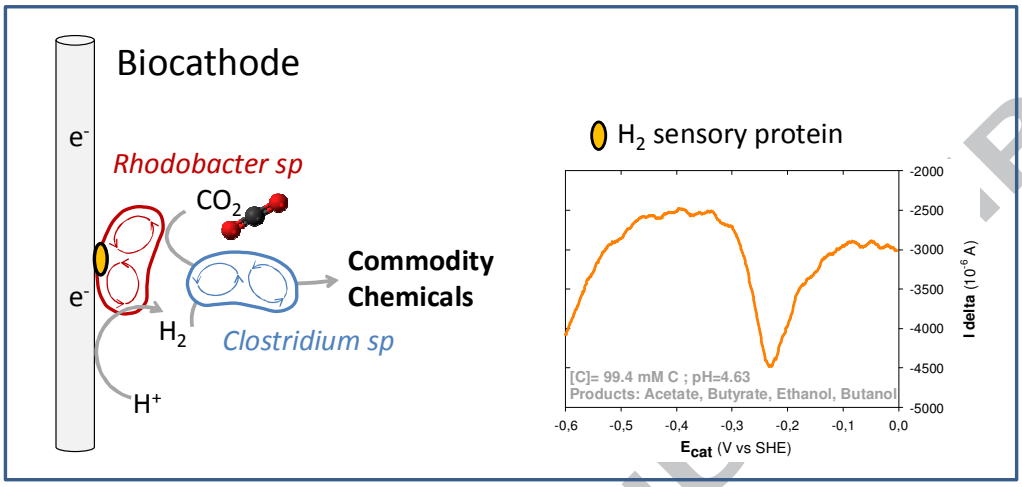

Highlights

1) Microbiome function is compartimentalized in bioelectrocatalysed reduction of CO_2

   .

2) *Rhodobacter* sp. could produce H_2 from the cathode electrode.

3) This system could be tracked by the H_2 sensory protein activity in *Rhodobacter* sp.